



Investigation of Hydraulic Performance of Standard and Modified USBR Type III Stilling Basin Using Scale Modeling: A Case Study of Mohmand Dam Spillway, Pakistan

Hassan Raza¹ · Muhammad Kaleem Sarwar¹ · Faraz ul Haq¹ · Muhammad Atiq Ur Rehman Tariq¹ · Tariq Altaf² · Yasir Abduljaleel³

Received: 16 March 2023 / Accepted: 13 July 2023 / Published online: 3 August 2023
© The Author(s), under exclusive licence to Shiraz University 2023

Abstract

The stilling basins are used for dissipating the flow energy in spillways. The hydraulic performance of the stilling basin is dependent on the shape and dimension of the basin. The literature review indicates that the convergence of the side walls of the stilling basin enhances the efficiency of the stilling basin and stabilizes the jump within the basin. The research aimed to investigate the hydraulic performance of USBR type III stilling basin by modifying its standard geometry. The stilling basin of the Mohmand Dam spillway located on the Swat River; Pakistan was selected as a study area. The model was operated with parallel walls of stilling basin and by converging the walls of stilling basin from 1° to 5°. The results indicated that the efficiency of the hydraulic jump with converged wall stilling basin has improved as compared to parallel walls and loss of energy increased due to convergence. The efficiency of stilling basin increased up to 4% with the increment in wall convergence, but the optimum efficiency of the hydraulic jump was obtained at 3° wall convergence. The results also indicated that an increase in convergence angle leads to an increase in bottom pressures. Furthermore, the modified baffle blocks increased the energy dissipation efficiency to 1% as compared to standard baffle blocks. The study concludes that wall convergence not only improves the hydraulic performance of the stilling basin but also reduces the construction cost of the stilling basin.

Keywords Hydraulic jump · Energy dissipation · Stilling basin · Physical modelling

Abbreviations

Amsl	Above mean sea level	M _{4-F}	Free flow model operation at 4° wall convergence
CEWRE	Centre of Excellence in Water Resources Engineering	M _{5-F}	Free flow model operation at 5° wall convergence
Fr ₁	Froude number just before the hydraulic jump	M _{1-G}	Gated flow model operation at 1° wall convergence
M _{1-F}	Free flow model operation at 1° wall convergence	M _{2-G}	Gated flow model operation at 2° wall convergence
M _{2-F}	Free flow model operation at 2° wall convergence	M _{3-G}	Gated flow model operation at 3° wall convergence
M _{3-F}	Free flow model operation at 3° wall convergence	M _{4-G}	Gated flow model operation at 4° wall convergence
		M _{5-G}	Gated flow model operation at 5° wall convergence
		M	Meter
		Q	Discharge
		USBR	United States Bureau of Reclamation
		WAPDA	Water and Power Development Authority
		°	Degree

✉ Hassan Raza
hassanrazahrj@gmail.com

¹ Centre of Excellence in Water Resources Engineering, University of Engineering and Technology, Lahore 54890, Pakistan

² Levant Consultant, Lahore, Pakistan

³ Department of Civil and Environmental Engineering, Washington State University, Richland, WA 99354, USA

1 Introduction

Whenever the flow depth changes from a low depth to a high depth due to a reduction in the velocity, then the water surface rises, this phenomenon is known as a hydraulic jump. Hydraulic jumps are commonly used as energy dissipaters. To bring the flow of water to a normal state, it is essential to facilitate the dissipation of kinetic energy at the toe of a spillway (Khatsuria 2004). An effective way for decreasing the exit velocity of water to a mild state is using a hydraulic-jump type stilling basin. The purpose of the stilling basin is to contain a hydraulic jump within a confined geometry to control the high energy flows entering the basin and its energy dissipation within a hydraulic jump. Stilling basins consist of horizontal or sloping floor beds having auxiliary devices such as chute blocks, baffle blocks, and end sills. These auxiliary devices affect up to 60% loss of the energy within the basin depending upon the Froude number of the flow (Ali 2003).

Over the past year, several studies and investigations have been done to test and validate the performance of various elements (chute and baffle blocks) in a stilling basin to contribute to a shorter more efficient basin. As mentioned (De Padova and Mossa 2021), George Bidone (1781–1839) was the first to perform experiments on the hydraulic jump phenomenon in 1818. Peterka (1984) suggested a stilling basin with chute blocks and a solid end sill which maximizes its performance without making the structure over-costly. Peterka (1984) stated that auxiliary devices such as chute blocks, baffle blocks, or increased floor bed length are somewhat productive in maintaining the tailwater depth. Likewise, a shorter floor bed length cannot be adjusted by an additional tailwater depth. Later research by USBR (1978) suggested a short stilling basin, with chute blocks, baffle piers, and a dented end sill. Many researchers have contributed to chute block and baffle block design suggesting various types and layouts of chute blocks and baffle blocks to maximize energy dissipation and minimize the risk of cavitation (Pillai et al. 1989).

The baffle block design was developed by the (United States Army Corps of Engineering 1992) in a model study for the Libby Reregulating Dam in the USA. 3 m high baffle blocks were placed about 5.5 m apart in the flow direction and 1.5 m apart in the transverse direction on a 25 m high spillway chute. These baffle piers are said to have been excellent in dissipating energy as well as aeration of the flow. The baffles blocks worked efficiently in the 80 m³/s/m unit discharge. Frizell and Svoboda (2012) investigated stilling basin downstream of the converging stepped spillway. The 40-m-long stilling basin was tested with and without the designed end sill. Removal of the designed end sill produced poor flow conditions in the

basin and thus basin with an end sill was adopted, which produced excellent flow conditions and energy dissipation.

Long et al. (1991) investigated the performance of a submerged hydraulic jump to predict the mean flow and turbulence properties of the submerged jump. It was found that the model was suitable for predicting the surface profile, the mean velocity, and the turbulence of submerged hydraulic jumps. Ohtsu et al. (1991) explained the result of a continuous end sill on the hydraulic jump. Hager (1992) studied different types of energy dissipation hydraulic structures and standardized stilling basins and hydraulic jumps. Results indicated that higher Froude number values (4.5–9) stabilized the hydraulic jump which led to an optimal loss of energy in the basin.

Yang (1994) designed a device known as a "dispersive-flow energy dissipator." In comparison with the traditional design of the stilling basin to accommodate the discharge, the results indicated that the hydraulic performance of the new dissipator was better than the traditional energy dissipation techniques. The new dissipator reduced the basin length by 50–66% and less tailwater depth was required; hence the construction cost was reduced. The dissipator is suited for heads of 50–80 m.

Ead and Rajaratnam (2002) investigated the influence of the ridged bed on a hydraulic jump and concluded that the hydraulic jump length was reduced by 50%. Furthermore, shear stress on the ridged bed was about ten times high than on a plane bed. Jumps length were reduced to 50% on ridged beds compared to jumps on plane beds. Omid et al. (2007) studied hydraulic jump in a converged rectangular channel for divergence angles of 5° and 7° and different lateral slopes at different discharges. The result showed the hydraulic jump length decreased and the percent of relative energy dissipation increased in the converged rectangular channel. Lueker et al. (2008) conducted a physical model study to investigate the performance of the designed stilling basin for different flow conditions and determine if the stepped spillway or the stilling basin was prone to cavitation damages at discharges equal to or less than the design flow. The scale model tests showed that the designed basin was unable to keep the hydraulic jump within the basin under design flow conditions. Therefore, the basin length was increased up to 76 m, and the two baffle rows and an end sill were replaced. As a result, 80% of energy dissipation was reported immediately downstream of the modified stilling basin under the design flow condition, of which 55% was attributed to the stepped chute.

Alikhani et al. (2010) investigated the influence of vertical sill on energy dissipation. Results indicated that by using an end sill, the length of the stilling basin was lessened up to 30% by forced jumps compared with a free jump. Pirestani et al. (2011) observed the loss of energy by converging the stilling basin walls. Results indicated that convergence

caused an increase in loss of energy and hydraulic performance of the basin enhanced, 5° convergence of wall showed the best performance. Gharehbaba (2013) examined the efficiency of impact blocks during a submerged jump that occurs in a stilling basin. The results revealed that the presence of the baffle blocks in a submerged hydraulic jump can enhance energy dissipation. Efficiency was higher with baffle blocks than that without baffle blocks.

Valero et al. (2015) studied relations between chute blocks and extremely aerated flows inside stilling basin. By the varying height of chute blocks, contact between aerated flows and chute blocks was studied. The experimental data for the naturally aerated flow in the spillway and the sloping hydraulic jump showed positive results. Akib et al. (2015) investigated the properties of hydraulic jumps for 3 different shapes of ridged beds in a rectangular channel. Circular-shaped, rectangular, and triangular tire waste ridged beds were used. Results indicated that by using such corrugated beds, the length of the hydraulic jump was lessened up to 11, 10, and 7% respectively. Tail water depth was also reduced up to 11.5% by the corrugated bed. The corrugated bed's physical properties decreased the hydraulic jump's relative height and length.

Amorim et al. (2015) examined the flow inside a hydraulic jump stilling basin using a physical model and computational fluid dynamics codes. The numerical model exhibited satisfactory results with the experimental model, indicating the viability of this sort of modeling for modifying stilling basins. Babaali et al. (2015) physically investigated the flow in a United States Bureau of Reclamation (USBR) type II stilling basin by converging the side walls of stilling basin at four different converging angles (5° , 7.5° , 10° , and 12.5°) and compared the results with the numerical model. The results indicated that hydraulic jump performance in the stilling basin with convergent side walls was much better than the stilling basin with parallel side walls. By converging the side walls of the stilling basin, not only the hydraulic jump stabilized within the basin, but energy loss also increased within the stilling basin. The best convergent angle for the dissipation of energy in the stilling basin was 5° . Elsaheed et al. (2016) investigated how geometrically different stilling basin and end step heights influenced the performance of submerged hydraulic jumps and energy loss. Results indicated that the energy loss near the bed increased up to 25% by increasing the Froude number by around 50%.

Valero et al. (2016) estimated the hydraulic performance of USBR type III stilling basin downstream of the stepped and ogee spillways. Results indicated that when the model was operated with a stepped chute, the flow was highly turbulent throughout the spillway chute causing maximum energy dissipation within the basin. Because the entrance flow was far more turbulent than that of a smooth chute, the steps caused an even greater decrease in the maximum

velocity within the basin. Additionally, baffle blocks encouraged maximum velocity decay, which demonstrated the higher hydraulic performance of the stilling basin.

Water and Power Development Authority—Wapda (2017) physically examined the hydraulic performance of spillway and energy dissipation in a double stilling basin (upper and lower basins) model in a standard USBR type III stilling basin. The model was tested with modified baffle blocks. The results indicated that in the basic design of the upper stilling basin, hydraulic jump swept out of the basin at higher discharges but after modification (location and size of baffle blocks, aerator height, and length of the basin), jump contained within the basin. In the lower stilling basin with a floor elevation of 355.5 m amsl, the hydraulic jump swept out at a reservoir elevation of 555 m amsl. However, in the modified design by lowering the basin elevation to 348 m amsl the hydraulic jump contained within the basin. Abbas et al. (2018) studied the effect of baffle block configuration on the behavior of hydraulic jump in the stilling basin using physical modeling. The result indicated that the baffle block caused a decrease in the jump length ratio and a decrease in the length of the roller, but the energy dissipation ratio increased. Babaali et al. (2018) physically examined the static pressures in a USBR type II stilling basin by conducting the experiments in parallel and converging side walls of stilling basin with 5° , 7.5° , 10° and 12.5° converging angles and compared the results with numerical model. The results indicated the best stilling basin regarding static pressure was converging stilling basin. Furthermore, static pressure was increased by increasing the converging angle and improved the hydraulic performance of stilling basin.

Torkamanzad et al. (2019) investigated the effects of the expansion and the roughness height on the main properties of the jump through laboratory experiments. The study revealed that the main parameters of the jump are a function of the upstream Froude number. It is noteworthy to mention, the bed roughness enhanced the energy dissipation by the generation of large eddies and subsequently increased the bed shear stress and decreased the asymmetry and stabilized the hydraulic jump. Experimental observations showed that the spatial jump on an abruptly expanding basin is asymmetric and unstable, especially at high upstream Froude numbers, which brings about major difficulties in hydraulic jump control. The analysis of energy dissipation efficiency confirmed that the spatial jump in the abruptly expanded basin with the roughened bed was more efficient than the classical jump.

Mousavi et al. (2022) predicted the pressure fluctuations coefficient (C'_p) along the submerged and free jumps at the bottom of the USBR Type II stilling basin, based on the geometric and hydraulic parameters. Salmasi and Abraham (2022) studied and experimentally investigated the stilling basin invert elevation concerning the elevation

of the upstream water, the design discharge, and the elevation of the downstream water and tailwater.

The literature indicated that different techniques were applied to different projects around the globe to enhance the hydraulic performance of stilling basins. Researchers modified the standard geometry of the stilling basins to enhance the energy dissipation in the stilling basin. The objective of this study was to conduct experimental research on the energy dissipation in the USBR Type III stilling basin to assure the hydraulically efficient and cost-effective design of the stilling basin. In this study, the performance of hydraulic jump was investigated using different types of baffle blocks (standard baffle blocks and modified baffle blocks) in the USBR type III stilling basin. Moreover, the hydraulic performance of the USBR type III stilling basin was investigated by modifying the geometry of the basin (by converging the side walls of stilling basin at different angles) and by modifying the shape of the baffle blocks. For this purpose, a two bays physical model of the Mohmand dam spillway and stilling basin was constructed based on Froude number similarity criteria between the model and prototype using a geometric similarity ratio of 1:100.

1.1 Stilling Basin and Its Types

Stilling basin is an arrangement in which the energy of the flowing water is dissipated. A properly designed stilling basin does not merely enhance the energy dissipation of a hydraulic jump, but it may stabilize the hydraulic jump and reduce the length of the stilling basin. Hydraulic jump-type stilling basins are used for the dam spillways in which most of the energy is dissipated by the hydraulic jump. A hydraulic jump can be stabilized in a stilling basin by using accessories such as chute blocks, baffle blocks, and end sill.

United States Bureau of Reclamation developed four different types of stilling basins.

1.1.1 Stilling Basin Type I

This is a simple stilling basin with a horizontal bottom and no appurtenances.

1.1.2 Stilling Basin Type II

The Type II stilling basin is used on concrete and earth dam spillways. It is used where the upstream Froude number is greater than 4.5. This stilling basin consisted of chute blocks and a dentated end sill only which may reduce the stilling basin length by 33%.

1.1.3 Stilling Basin Type III

The Type III stilling basin is used for gravity and earth dam spillways. It is also used where the upstream Froude number is greater than 4.5. This stilling basin consisted of chute blocks, baffle blocks, and an end sill which may reduce the stilling basin length by 45–60%. Baffle blocks are used to limit the inflow velocities to avoid cavitation damage to the concrete surface of the stilling basin bed.

1.1.4 Stilling Basin Type IV

The Type IV stilling basin is used on canal structures and diversion canals. It is used where the upstream Froude number is between 2.5 and 4.5. This stilling basin consisted of chute deflector blocks and a continuous end sill.

The reason for selecting the USBR type III stilling basin is that it is a case study of the Mohmand dam spillway. USBR Type III is used in the prototype so does in the model. Mohmand Dam spillway has a double arrangement of stilling basins due to the high head and both stilling basins are USBR type III. Moreover, the Mohmand Dam spillway has a head of more than 200 m and there is high cavitation occurring in the basin so USBR type III has baffle blocks to reduce the cavitation.

2 Study Area

Mohmand Dam is located on the Swat River, in Mohmand Agency of Pakistan shown in Fig. 1. Spillway is constructed on the left side of the dam to pass the design flood of 27,427 m³/s. Spillway consisted of seven bays and two long concrete chutes and two stilling basins are provided to dissipate the energy. The plan and profile of Mohmand dam spillway is shown in Figs. 2 and 3.

3 Materials and Methods

3.1 Dimensional Analysis

Dimensional analysis was carried out to determine the significance of parameters to be considered in investigating flow through spillways. The Buckingham II theorem has been adopted in the present study to understand the dimensional analysis of the spillway flows. The flow through the spillway is characterized by various hydraulic parameters such as density ρ (kg/m³), dynamic viscosity μ (N s/m²), surface tension σ (N/m), acceleration due to gravity g (m/s²), velocity of flow v (m/s), head over the crest h_d (m), pressure head h_p (m), flow depth y (m), specific energy E (m), energy loss ΔE (m).

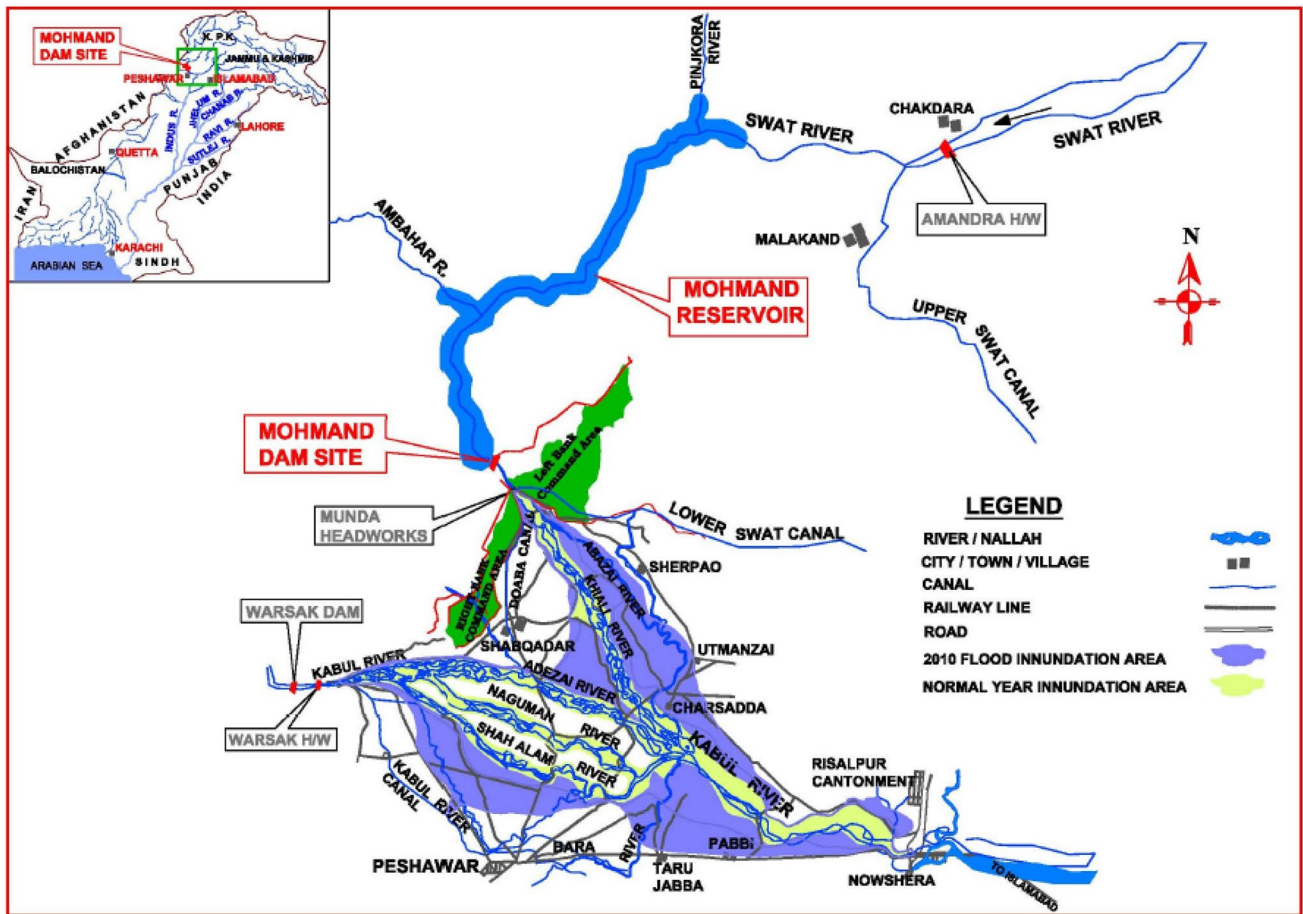


Fig. 1 Location of Mohmand Dam project (Source: Water and power development authority—Wapda 2017)

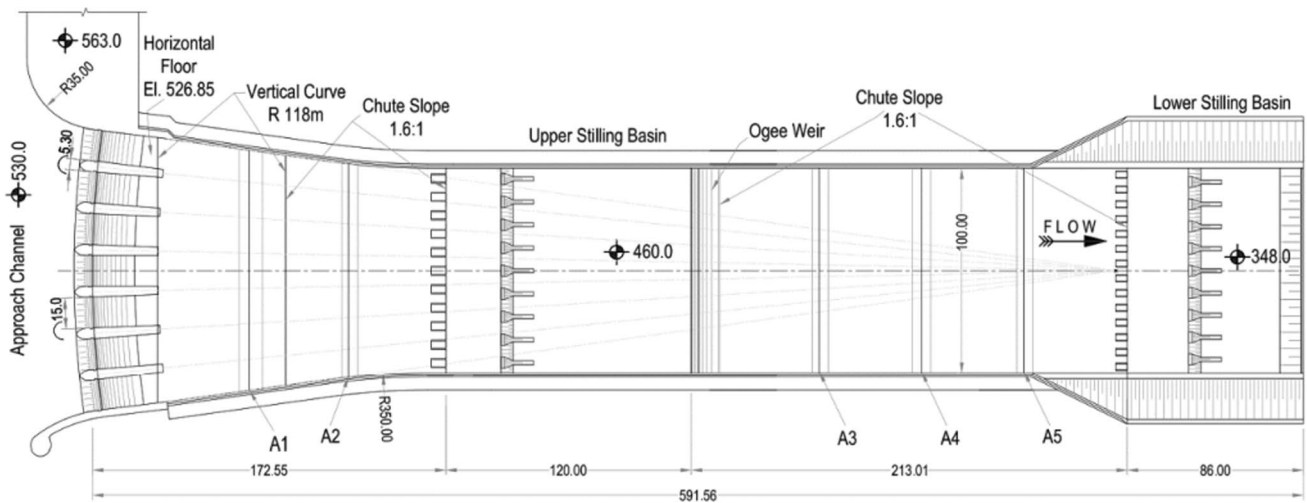


Fig. 2 Plan of Mohmand Dam spillway (Source: Water and Power Development Authority—Wapda 2017)

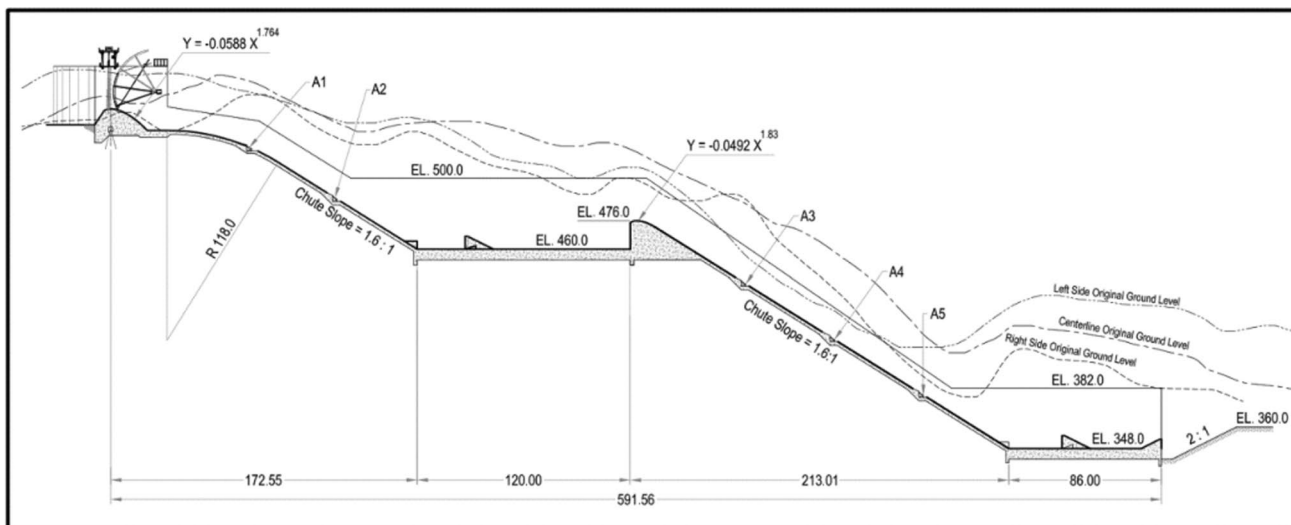


Fig. 3 Profile of Mohmand Dam spillway (Source: Water and Power Development Authority—Wapda 2017)

Taking into account all the above parameters, the following dimensional group was formed as given in Eq. 1.

$$f(\rho, \mu, \sigma, g, v, h_d, h_p, y, E, \Delta E) = 0 \tag{1}$$

Using the Buckingham Π theorem and rearranging all the parameters, Eq. 2 was obtained.

$$f\left(\frac{\mu}{\rho v y}, \frac{\sigma}{\rho v^2 y}, \frac{g y}{v^2}, \frac{E}{y}, \frac{\Delta E}{y}, \frac{h_d}{y}, \frac{h_p}{y}\right) = 0 \tag{2}$$

It is convenient to invert the parameters and introduce the dimensionless parameters Froude number Fr , Reynolds number Re , and Weber number We ,

Equation (2) can be written as given in Eq. 3.

$$f\left(Fr, Re, We, \frac{y}{E}, \frac{y}{\Delta E}, \frac{y}{h_d}, \frac{y}{h_p}\right) = 0 \tag{3}$$

3.2 Dynamic Similarity

For the dynamic similarity between model and prototype the ratio of corresponding forces acting at the corresponding points in the model and prototype should be equal. The Froude law represents the condition of dynamic similarity for flow in the model and prototype governed by gravity and inertia force. Other forces such as the frictional resistance of a viscous liquid, and the forces of volumetric elasticity, either don't affect the flow or their effect may be neglected. Gravity is the predominant force in free surface flows such as flow over spillways, weirs, sluices, channels, etc. Therefore, spillway models are based on the Froude scaling and the scale of the model is chosen in such a way

that the scale effects are minimum due to non-similarity of the Reynolds and Weber numbers. In this study, Froude's model law was used.

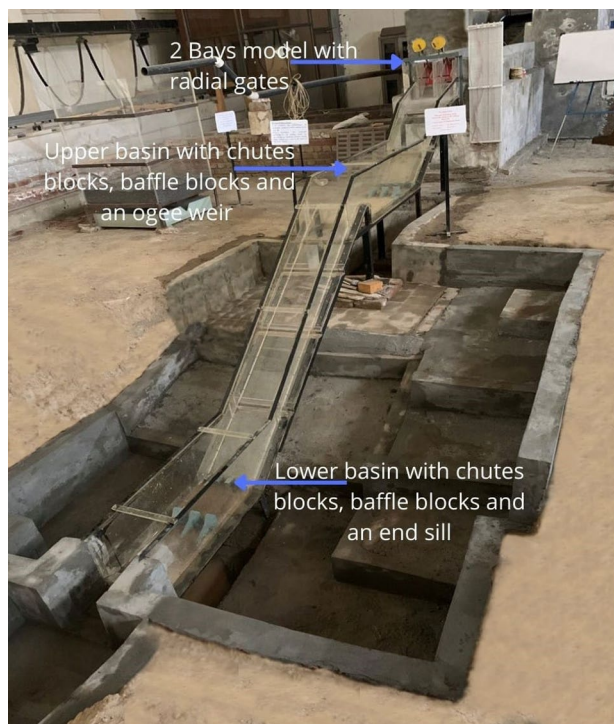


Fig. 4 Physical model of Mohmand Dam spillway and stilling basin

3.3 Experimental Setup

A physical model of the Mohmand Dam spillway was constructed in the model tray hall of the Center of Excellence in Water Resources Engineering (CEWRE), Lahore, Pakistan as shown in Fig. 4. The model was designed based on Froude number similarity criteria. It was constructed with two bays only at a scale of 1:100 considering discharge and space limitations.

The Spillway model with two gated bays was installed in front of the V-notch water tank. The crest level of the model was considered as a benchmark i.e., 539 m amsl. Then the remaining part of the model having two spillway chutes and two stilling basins was installed. Auto-level was used to set the reduced levels of the upper stilling basin, lower stilling basin, and riverbed level. A channel was constructed downstream of the model and a tailgate was installed at the end of the channel to maintain the tailwater level. Two gauges were installed, one near to tailgate and the second one in the middle of the riverbed channel to observe and maintain the tailwater level. After installing the tailgate at the end of the channel, a conveyance channel was prepared to discharge out the water towards recirculating channel (main channel) of the model tray hall. In addition to the installation of the spillway model, V-Notch, stilling well with a point gauge and piezometers for pressure measurements was also installed at a model site in the model tray hall.

To observe the water head above the spillway crest, Reservoir levels were marked on the inside wall of the reservoir tank as shown in Fig. 5.

To observe the discharge for the model, a V-Notch was placed in front of the water tank and a gauge well was installed at the right-side wall of the water tank. The gauge well provides water level measurement relative to the bottom



Fig. 5 Reservoir levels marked on the inside wall of the tank

of V-Notch with the help of a point gauge. The gauge well as a transparent vessel made of Plexiglas. It receives water from the tank through a 0.5-inch diameter pipe. The water head so measured was used in the discharge formula for V-Notch to calculate the discharge given in Eq. 4.

$$Q = 1.37H^{2.5} \quad (4)$$

where Q is the discharge in m^3/s and H is the water head upstream of V-Notch in m.

Velocity was measured (three-point velocity method) by the current meter upstream of a hydraulic jump, downstream of a hydraulic jump, and at tail water level. For flow depth observation, five no. of locations were marked, two within the model, (upstream of the hydraulic jump and downstream of the hydraulic jump), and the other three observations were downstream to the model. Flow depth was measured by a point gauge. To observe the pressure head, piezometers were installed just near the model. Pressure heads were observed at three different locations in the stilling basin, i.e., at the start of the basin, at baffle blocks, and near the end sill. By observing these flow parameters, Froude number, length of the jump, specific energy up-stream and down-stream of the jump, loss of energy, and efficiency of the hydraulic jump were computed.

3.4 Model Validation

The validation was done between the observed and computed values of the discharge for free and gated flows discussed in Table 1. Computed values were taken from the Detailed Design Report of the Mohmand Dam Hydropower Project while the observed values of discharge were taken from the model.

3.5 Model Operating Conditions

To evaluate the performance of the hydraulic jump in the stilling basin III, initially model was operated at standard geometry (without converging the walls of stilling basin) with standard and modified baffle blocks by varying the

Table 1 Observed and computed discharges comparison

Sr. no	Reservoir levels amsl (m)	Observed discharge (m^3/s)	Computed discharge (m^3/s)	Error %
1	539	0	0	0
2	542	1075	1039	3.34
3	544	2239	2199	1.77
4	548	5789	5695	1.62
5	551	8980	8744	2.62

Table 2 Model operating condition for free and gated flows with standard stilling basin

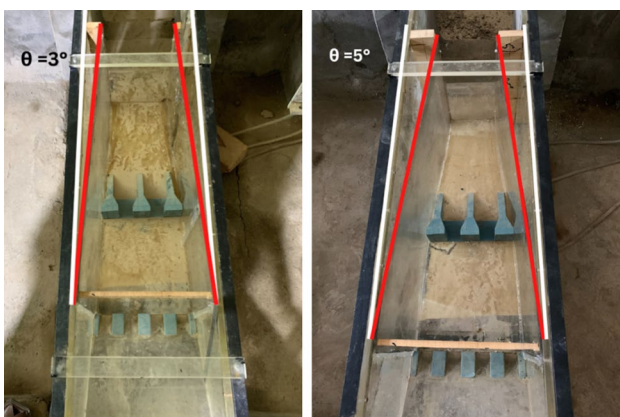
Model operating conditions with parallel walls of stilling basin (0°)			
Flow condition	Reservoir levels (m)	Flow condition	Gate lip levels (m)
Free flow	542	Gated flow with maximum reservoir level set at 558 m amsl	542
	544		544
	548		548
	551		551

Table 3 Model operating conditions for free flows at modified stilling basin geometry

Operating conditions		Models with converged walls of stilling basin and modified shape of baffle blocks				
Flow condition	Reservoir levels amsl (m)	M _{1-F}	M _{2-F}	M _{3-F}	M _{4-F}	M _{5-F}
Free flow	542	1°	2°	3°	4°	5°
	544	1°	2°	3°	4°	5°
	548	1°	2°	3°	4°	5°
	551	1°	2°	3°	4°	5°

Table 4 Model operating conditions for gated flows at modified stilling basin geometry

Operating conditions		Models with converged walls of stilling basin and modified shape of baffle blocks				
Flow condition	Gate lip levels amsl (m)	M _{1-G}	M _{2-G}	M _{3-G}	M _{4-G}	M _{5-G}
Gated flow with maximum reservoir level set at 558 m amsl	542	1°	2°	3°	4°	5°
	544	1°	2°	3°	4°	5°
	548	1°	2°	3°	4°	5°
	551	1°	2°	3°	4°	5°

**Fig. 6** Stilling basin models with converged walls at 3° and 5° respectively

reservoir levels for free and gated flow conditions. The details of the model's operating conditions are discussed in Table 2.

Later, the geometry of the USBR type III stilling basin was modified. To investigate the hydraulic performance of stilling basin, the side walls of stilling basin were converged at different angles discussed in Tables 3 and 4. The side walls of the stilling basin converged up to 5° (starting from 1° with an increment of 1°) as shown in Fig. 6. In this way, five models were developed with converged walls. Each model was operated for free and gated flow conditions by varying the reservoir levels.

By measuring flow depth and flow velocity, the Froude number was computed which describes whether the flow is supercritical or subcritical. Furthermore, flow depth and flow velocity were also helpful in finding the efficiency of the hydraulic jump and the loss of energy. The water surface levels were observed to check whether the flow is contained within the stilling basin or not.

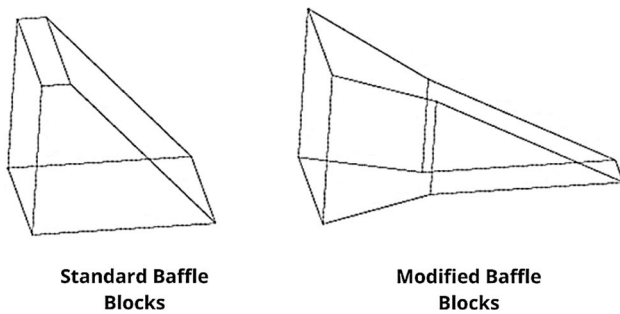


Fig. 7 Geometry of standard and modified baffle blocks

4 Results and Discussions

4.1 Performance Evaluation of Hydraulic Jump with Standard Geometry of Stilling Basin

The hydraulic performance of the jump was investigated in the standard stilling basin geometry with two types of baffle blocks (standard and modified baffle blocks). Figure 7 is a pictorial representation of both types of baffle blocks. For this purpose, the model was operated by varying the reservoir level for free flow and gated flow conditions described earlier.

At the chute, pre-jump velocities were significantly higher than post-jump velocities shown in post-jump flow velocities were less, and post-jump flow depths were high in modified baffle blocks as compared to standard baffle blocks shown in Fig. 8. It is due to the reason that modified baffle blocks were more efficient in breaking the kinetic energy of flow which is entering the stilling basin due to its impact action. Hence more energy was dissipated by using modified baffle blocks and so the velocity of the flow was reduced, and flow depth increased. The same results were observed in the model with the gated flow operation.

At the chute, less flow depths were observed just before the hydraulic jump but in the stilling basin after

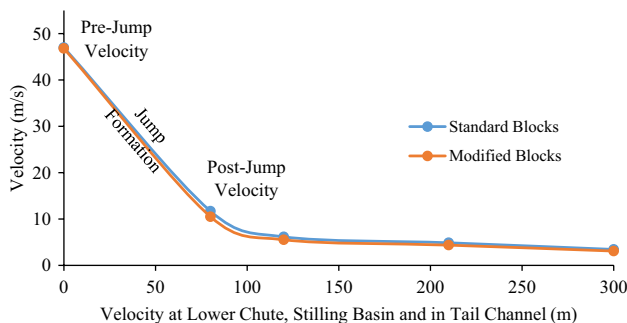


Fig. 8 Flow velocity with standard and modified baffle blocks

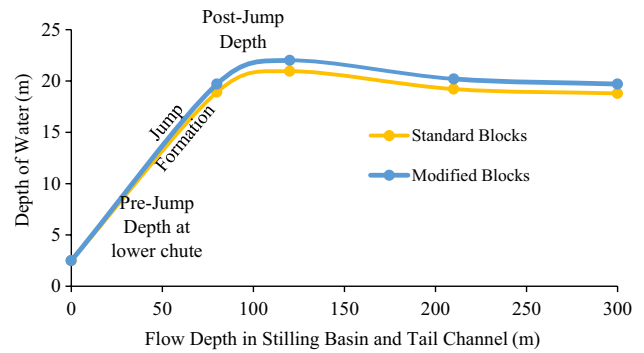


Fig. 9 Flow depth with standard and modified baffle blocks

the hydraulic jump formation, it was considerably high in both types of flows (free and gated flows) due to the flow being converted from supercritical flow to subcritical flow. Flow depth was found to be smooth downstream of the model in both types of flows as shown in Fig. 9.

In the case of dam spillways, Froude number of incoming flows lies between 4.5 and 9, and the jump so the form is a steady jump, and its performance is at its best. The Froude number was calculated using Eq. 5. Froude numbers at the chute have more value due to higher velocities of the flow than inside of the stilling basin. In all the experiments, the subcritical flow was observed at the inside of the stilling basin in which the Froude number is less than 1 and supercritical flow was observed at the chute where the Froude number is greater than 1. Post-jump Froude number values were less in modified baffle blocks as compared to standard baffle blocks due to reduced post-jump velocities with modified baffle blocks.

$$Fr = \frac{(v)^2}{gy} \tag{5}$$

where Fr is the Froude number of the flow, v is velocity of the flow in m , y = flow depth in m and g is the gravitational acceleration in m/s^2 .

The efficiency of the jump shows how much energy is dissipated within the basin. Jump efficiency was calculated using Eq. 6 described below and it was high in the case of modified baffle blocks as compared to standard USBR baffle blocks in both operating conditions (free and gated flow conditions). Maximum efficiency was observed at 551 m amsl in both operating conditions. Figure 10 shows the efficiency of the jump.

$$\eta = \frac{(E_1 - E_2)}{E_1} * 100 \tag{6}$$

where E_1 is the specific energy just before the hydraulic jump in m , E_2 is the specific energy after the formation of

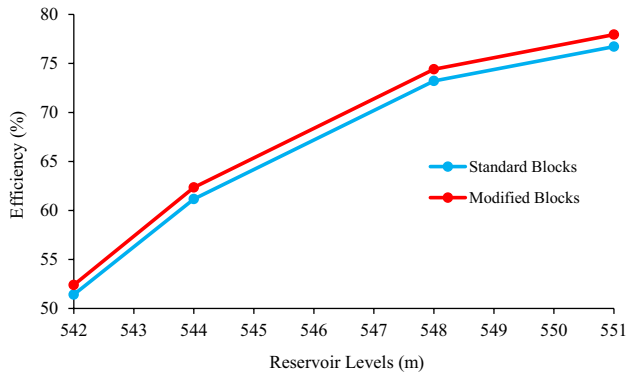


Fig. 10 Hydraulic jump efficiency with standard and modified baffle blocks

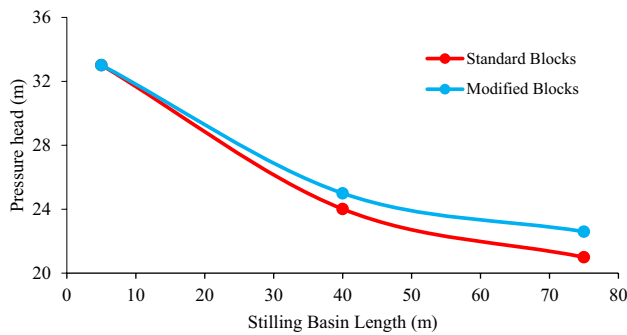


Fig. 11 Pressure head with standard and modified baffle blocks

hydraulic jump in m and η is the efficiency of the hydraulic jump.

Specific energy was calculated using the Equation below.

$$E_1 = y_1 + \frac{v_1^2}{2g} \tag{7}$$

$$E_2 = y_2 + \frac{v_2^2}{2g} \tag{8}$$

In the specific energy, flow depth was measured by using a point gauge, and velocity was measured using the current meter. Energy loss in the hydraulic jump was computed by Eq. 9. Energy loss was high in the case of modified baffle blocks.

$$\Delta E = \frac{(y_2 - y_1)^3}{4y_2y_1} \tag{9}$$

where y_1 is the flow depth just before the hydraulic jump in m, y_2 is the flow depth after the formation of hydraulic jump in m and ΔE is the loss of energy.

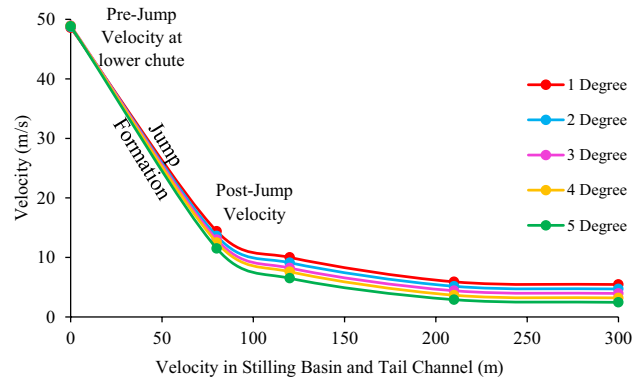


Fig. 12 Flow velocities with stilling basin walls converged at different angles

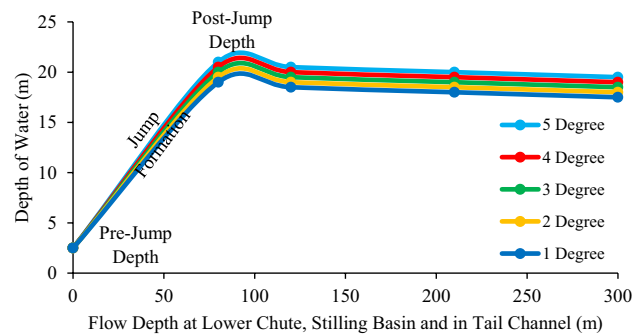


Fig. 13 Flow depths with stilling basin walls converged at different angles

Pressure values were high in the case of modified baffle blocks as compared to standard USBR baffle blocks as shown in Fig. 11 which was a good indication for an increase in energy dissipation and hence improved the performance of jump with modified baffle blocks.

4.2 Performance Evaluation of Hydraulic Jump with Modified Geometry of Stilling Basin

Under this scenario, the performance of the hydraulic jump was assessed by converging the side walls of the stilling basin at different angles and placing the modified shapes of the baffle blocks. The model was operated as discussed earlier in model operations.

In Fig. 12, Pre-jump flow velocities were almost the same but post-jump flow velocity decreased by converging the walls of the stilling basin. A higher converging angle caused a further decrease in the velocity. Flow depths with stilling basin walls converged at different angles are shown in Fig. 13.

For free flow model operations, it was observed that at all the discharges water level did not overtop the side walls

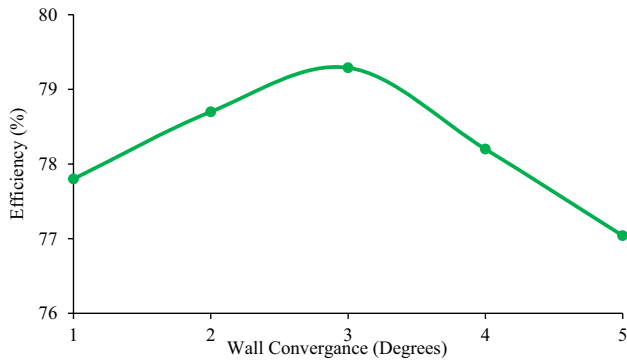


Fig. 14 Efficiency of hydraulic jump at R.L. 551 m asl (free flow condition)

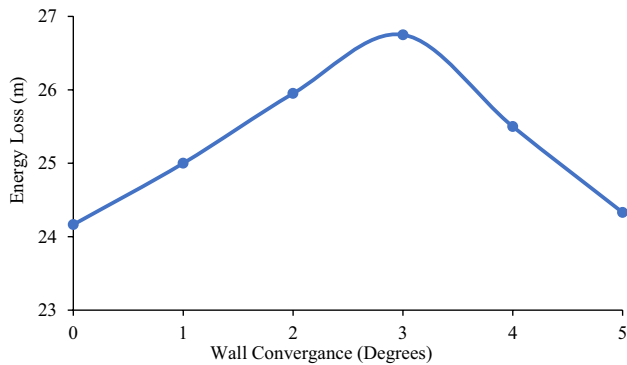


Fig. 15 Energy loss with stilling basin walls converged at different angles

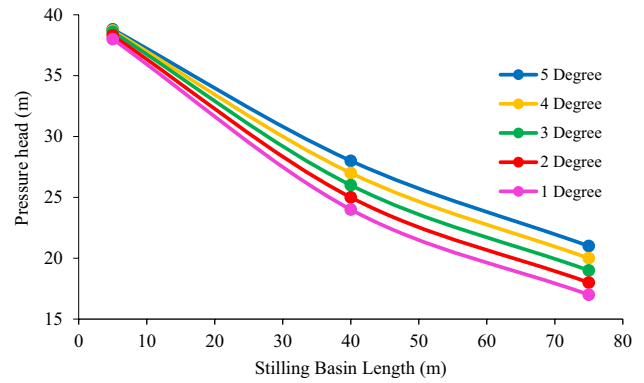


Fig. 16 Pressure head variation with stilling basin walls converged at different angles

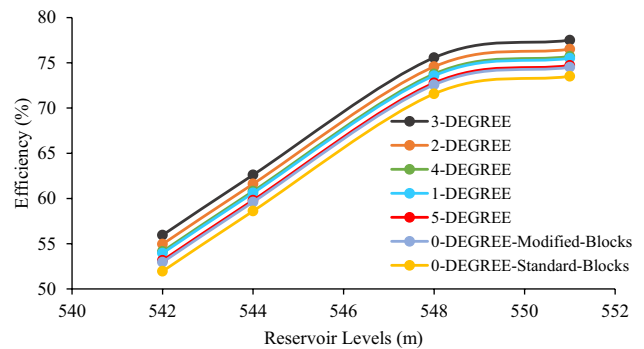


Fig. 17 Comparison of hydraulic jump efficiency for all the testing scenarios

of the basin by converging the stilling basin. Whereas in gated flow model operations at high reservoir levels such as 548 m amsl and 551 m amsl water overtops the side wall of the basin. Post jump Froude number decreased as the Froude number is directly proportional to the velocity. In all the experiments, the supercritical flow was observed at the chute, and subcritical flow was observed inside the stilling basin and at the tail channel. Moreover, jump efficiency increased by increasing the converging angle of stilling basin walls up to 3° as shown in Fig. 14. At 4° and 5° converging angles of the stilling basin walls, the efficiency of the jump was reduced due to the increase in flow depth.

Energy Loss increased by increasing the converging angle of the side walls of the stilling basin up to 3° but then decreased due to an increase in the post-jump flow depth as shown in Fig. 15.

Pressure heads were also measured in the modified geometry of stilling basin. The results indicated that an increase in the converging angle led to increasing the pressure as shown in Fig. 16.



Fig. 18 Free flow model operation with 5° wall convergence

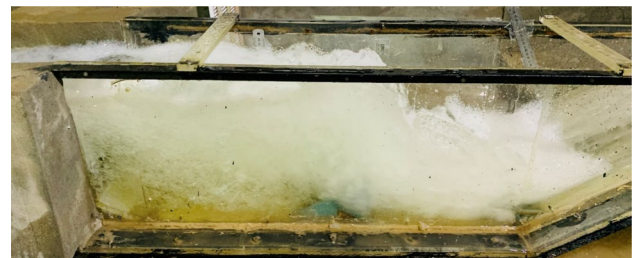


Fig. 19 Model operation with parallel walls

4.3 Comparison of the Hydraulic Jump Efficiency for all the Testing Scenarios

Figure 17 shows the jump efficiency for all the testing scenarios while Figs. 18 and 19 shows free flow model operation with 5° wall convergence and model operation with parallel walls. In all the testing scenarios, the efficiency of the jump was higher at 3° convergence of stilling basin walls with modified baffle blocks.

5 Conclusions and Recommendations

A model study was conducted on a Mohmand Dam spillway with different operating conditions. The focus of the study was to investigate the hydraulic performance of USBR type III stilling basin by modifying the geometry of the stilling basin and modifying the shape of baffle blocks. To contain the hydraulic jump within the stilling basin and to increase the energy dissipation phenomenon, the side walls of the stilling basin converged from 1° to 5°. The model was operated for free and gated flow conditions. Initially, the model was tested at standard stilling basin geometry with both types of blocks (standard and modified baffle blocks). The results indicated that the hydraulic efficiency of the USBR type III stilling basin was 1% high by placing the modified baffle blocks as compared to standard USBR baffle blocks. Pressure heads were 4% high with modified baffle blocks. Then the geometry of the stilling basin was modified. The model was operated by converging the side walls of the basin with modified baffle blocks. At all the operating conditions, converged walls improved the hydraulic performance of the stilling basin up to 3°. Maximum energy dissipation was observed at 3° wall convergence but at higher wall convergence (4° and 5°) it decreased due to an increase in the flow depth at the end of the basin. Pressure heads increased up to 8% by increasing the converging angles of the walls. The study concluded that wall convergence not only improved the hydraulic performance of the stilling basin but also reduced the construction cost of the stilling basin by containing the hydraulic jump within the basin.

The total length of Mohmand Dam's lower stilling basin is 86 m and its cost is 2.2 billion rupees. Through this study, an economy in the length of the basin with maximum energy dissipation was tried to achieve by modifying its standard geometry. By converging stilling basin walls at 3°, the cost of stilling basin reduces to 2.13 billion rupees, saving almost 70 million rupees. Hence, stilling basins with a converging wall was found to be economically feasible.

It is recommended to check the hydraulic performance of stilling basin at a higher model scale ratio with higher converging angles. Moreover, it is recommended that the stilling basin with converged walls option may be considered

for practical implication as it is hydraulically efficient and economically feasible.

Acknowledgements This study is supported by the (CEWRE) UET, Lahore, and the WAPDA model study cell, Nandipur, Gujranwala Pakistan.

Funding No funding was received for conducting this study.

Data Availability The data used in this study is available from the corresponding author on reasonable request.

Declarations

Conflict of interest The authors have no competing interests to declare that are relevant to the content of this article.

References

- Abbas A, Alwash H, Mahmood A (2018) Effect of baffle block configurations on characteristics of hydraulic jump in adverse stilling basins. *MATEC Web Conf* 162:03005. <https://doi.org/10.1051/mateconf/201816203005>
- Akib S, Ahmed A, Imran H et al (2015) Properties of hydraulic jump over apparent corrugated beds. *Dam Eng* 25:65–77
- Ali I (2003) Irrigation and hydraulic structures
- Alikhani A, Behrouzi-rad B, Moghadam MF (2010) Hydraulic jump in stilling basin with vertical end sill. *Int J Phys Sci* 5:25–29
- Amorim JC, Amante R, Barbosa C (2015) Experimental and numerical modeling of flow in a stilling basin. In: 26th IAHR world congress. IAHR, Hague
- Babaali H, Shamsai A, Vosoughifar H (2015) Computational modeling of the hydraulic jump in the stilling basin with convergence walls using CFD codes. *Arab J Sci Eng* 40:381–395. <https://doi.org/10.1007/s13369-014-1466-z>
- Babaali H, Soori N, Soori S et al (2018) Static pressure estimation on converging USBR II stilling basin: numerical approach. *Int J Sci Eng Investig* 7:2251–8843
- De Padova D, Mossa M (2021) Hydraulic jump: a brief history and research challenges. *Water* 13:1733. <https://doi.org/10.3390/w13131733>
- Ead SA, Rajaratnam N (2002) Hydraulic jumps on corrugated beds. *J Hydraul Eng* 128:656–663. [https://doi.org/10.1061/\(ASCE\)0733-9429\(2002\)128:7\(656\)](https://doi.org/10.1061/(ASCE)0733-9429(2002)128:7(656))
- Elsaeed G, Ali A, Abdelmageed N, Ibrahim A (2016) Effect of end step shape in the performance of stilling basins downstream radial gates. *J Sci Res Rep* 9:1–9. <https://doi.org/10.9734/JSRR/2016/21452>
- Frizell KW, Svoboda CD (2012) Performance of type III stilling basins—stepped spillway studies. *Hydraul Lab Rep* 25
- Gharehbaba AH (2013) Experimental study of submerged hydraulic jumps with baffle blocks. University of Alberta (Canada)
- Hager WH (1992) Energy dissipators and hydraulic jump, vol 8. Springer, Berlin
- Khatsuria R (2004) Hydraulics of spillways and energy dissipators
- Long D, Steffler PM, Rajaratnam N (1991) A numerical study of submerged hydraulic jumps. *J Hydraul Res* 29:293–308. <https://doi.org/10.1080/00221689109498435>
- Lueker ML, Mohseni O, Gulliver JS et al (2008) The physical model study of the Folsom Dam auxiliary spillway system. University of Minnesota, Minneapolis
- Mousavi SN, Farsadzadeh D, Salmasi F, Hosseinzadeh Dalir A (2022) Evaluation of pressure fluctuations coefficient along the USBR

- Type II stilling basin using experimental results and AI models. *ISH J Hydraul Eng* 28:207–214. <https://doi.org/10.1080/09715010.2020.1743208>
- Ohtsu I, Yasuda Y, Yamanaka Y (1991) Drag on vertical sill of forced jump. *J Hydraul Res* 29:29–47. <https://doi.org/10.1080/00221689109498991>
- Omid MH, Esmaeeli Varaki M, Narayanan R (2007) Gradually expanding hydraulic jump in a trapezoidal channel. *J Hydraul Res* 45:512–518. <https://doi.org/10.1080/00221686.2007.9521786>
- Peterka AJ (1984) Hydraulic design of stilling basins and energy dissipators, 4th edn. United States Department of the Interior. Bureau of Reclamation, Colorado
- Pillai NN, Goel A, Dubey AK (1989) Hydraulic jump type stilling basin for low Froude numbers. *J Hydraul Eng* 115:989–994. [https://doi.org/10.1061/\(asce\)0733-9429\(1989\)115:7\(989\)](https://doi.org/10.1061/(asce)0733-9429(1989)115:7(989))
- Pirestani MR, Razmkhah A, Ghobadi F (2011) Effect of convergent walls on energy dissipation in stilling basin by physical modeling. *Int J Therm Fluid Sci* 1:1–10. <https://doi.org/10.3923/ijtf.2012.1.10>
- Salmasi FF, Abraham J (2022) Determination of stilling basin invert elevation and its effect on controlling hydraulic jumps. In: Techniques and innovation in engineering research, vol 2. Book Publisher International (a part of SCIENCEDOMAIN International), pp 59–82
- Torkamanzad N, Hosseinzadeh Dalir A, Salmasi F, Abbaspour A (2019) Hydraulic jump below abrupt asymmetric expanding stilling basin on rough bed. *Water* 11:1756. <https://doi.org/10.3390/w11091756>
- United States Army Corps of Engineering (1992) Hydraulic design of spillways
- USBR (1978) Design of small dams
- Valero D, García-Bartual R, Marco J (2015) Optimisation of stilling basin chute blocks using a calibrated multiphase RANS model. In: Proc., 5th int. junior researcher and engineer workshop on hydraulic structures
- Valero D, Bung D, Crookston B, Matos J (2016) Numerical investigation of USBR type III stilling basin performance downstream of smooth and stepped spillways. In: International symposium on hydraulic structures. Portland, pp 652–663
- Water and Power Development Authority—Wapda (2017) Physical hydraulic model study—spillway model
- Yang SL (1994) Dispersive-flow energy dissipator. *J Hydraul Eng* 120:1401–1408. [https://doi.org/10.1061/\(ASCE\)0733-9429\(1994\)120:12\(1401\)](https://doi.org/10.1061/(ASCE)0733-9429(1994)120:12(1401))
- Springer Nature or its licensor (e.g. a society or other partner) holds exclusive rights to this article under a publishing agreement with the author(s) or other rightsholder(s); author self-archiving of the accepted manuscript version of this article is solely governed by the terms of such publishing agreement and applicable law.